Taxol-induced unfolded protein response activation in breast cancer cells exposed to hypoxia. ATF4 activation regulates autophagy and inhibits apoptosis

Notte, Annick; Rebucci, Magali; Fransolet, Maude; Roegiers, Edith; Genin, Marie; Tellier, Celine; Watillon, Kassandra; Fattaccioli, Antoine; Arnould, Thierry; Michiels, Carine

Published in:
International Journal of Biochemistry and Cell Biology

DOI:
10.1016/j.biocel.2015.02.010

Publication date:
2015

Document Version
Publisher's PDF, also known as Version of record

The International Journal of Biochemistry & Cell Biology 62 (2015) 1–14

Contents lists available at ScienceDirect

The International Journal of Biochemistry & Cell Biology

journal homepage: www.elsevier.com/locate/biocel

Taxol-induced unfolded protein response activation in breast cancer cells exposed to hypoxia: ATF4 activation regulates autophagy and inhibits apoptosis

Annick Notte [1], Magali Rebucci [1], Maude Fransolet, Edith Roegiers, Marie Genin, Celine Tellier, Kassandra Watillon, Antoine Fattaccioli, Thierry Arnould, Carine Michiels *

Laboratory of Biochemistry and Cellular Biology (URBC), NAmur Research Institute for Life Science (NARILIS), University of Namur, 61 rue de Bruxelles, 5000 Namur, Belgium

ARTICLE INFO

Article history:
Received 26 August 2014
Received in revised form 4 February 2015
Accepted 17 February 2015
Available online 24 February 2015

Keywords:
Breast cancer
Hypoxia
UPR
ATF4
Autophagy
Apoptosis

ABSTRACT

Understanding the mechanisms responsible for the resistance against chemotherapy-induced cell death is still of great interest since the number of patients with cancer increases and relapse is commonly observed. Indeed, the development of hypoxic regions as well as UPR (unfolded protein response) activation is known to promote cancer cell adaptive responses to the stressful tumor microenvironment and resistance against anticancer therapies. Therefore, the impact of UPR combined to hypoxia on autophagy and apoptosis activation during taxol exposure was investigated in MDA–MB-231 and T47D breast cancer cells. The results showed that taxol rapidly induced UPR activation and that hypoxia modulated taxol-induced UPR activation differently according to the different UPR pathways (PERK, ATF6, and IRE1α). The putative involvement of these signaling pathways in autophagy or in apoptosis regulation in response to taxol exposure was investigated. However, while no link between the activation of these three ER stress sensors and autophagy or apoptosis regulation could be evidenced, results showed that ATF4 activation, which occurs independently of UPR activation, was involved in taxol-induced autophagy completion. In addition, an ATF4-dependent mechanism leading to cancer cell adaptation and resistance against taxol-induced cell death was evidenced. Finally, our results demonstrate that expression of ATF4, in association with hypoxia-induced genes, can be used as a biomarker of a poor prognosis for human breast cancer patients supporting the conclusion that ATF4 might play an important role in adaptation and resistance of breast cancer cells to chemotherapy in hypoxic tumors.

1. Introduction

Resistance to chemotherapy is a major current issue in the outcome of cancer treatment. The mechanisms leading to drug resistance are complex and multifactorial. Although the inadequate drug concentration at the tumor site can contribute to clinical resistance, intrinsic cellular mechanisms or a reprogramming of the intracellular signaling pathways caused by the modifications of the tumor microenvironment contribute, for a major part, to drug resistance (Gatti and Zunino, 2005). One of these modifications is the presence of hypoxic areas in the tumor microenvironment of solid tumors. The responses induced by hypoxia result in cell adaptation and resistance to the chemotherapy-induced cell death. One of the most characterized transcription factors responsible for the hypoxic response is the hypoxia inducible factors (HIFs) (Semenza, 2010; Rohwer and Cramer, 2011). However, a number of HIF independent mechanisms are also able to promote cancer cell adaptation and survival and are of great interest to further improve cancer treatments and outcomes. (Rouschop and Wouters, 2009) In this work, two biological processes connected to cell death and/or stress adaptive responses have been investigated: autophagy and unfolded protein response (UPR).

Autophagy is a degradation process in which cells form double-membrane vesicles, called autophagosomes, sequestering a portion of cytoplasm. These autophagosomes ultimately fuse with lysosomes, resulting in the degradation of their content allowing the recycling of small molecules. Autophagy initiation

Abbreviations: ATF4, activating transcription factor 4; ATF6, activating transcription factor 6; ER, endoplasmic reticulum; IRE1α, inositol-requiring enzyme-1α; PERK, protein kinase double-stranded RNA-dependent (PRK)-like ER kinase; UPR, unfolded protein response.

* Corresponding author. Tel.: +32 81 724131; fax: +32 81 724135.
E-mail address: carine.michiels@unamur.be (C. Michiels).

[1] These authors contributed equally to this work.

http://dx.doi.org/10.1016/j.biocel.2015.02.010
1357-2725/

and completion requires mTOR (mammalian target of rapamycin) inhibition, the recruitment and activation of Vps34 (class-III phosphoinositide 3-kinase) within a protein complex containing beclin 1, several proteins encoded by Atg (Autophagy related genes) and two conjugation systems leading to Atg12–Atg5 as well as LC3-PE (PhosphatidylEthanolamine) conjugation (Mehrpour et al., 2010). In basal and activated conditions, autophagy contributes to the elimination of damaged organelles as well as to the turnover of long-lived proteins. In addition, autophagy can also be stimulated in response to different conditions of stress such as starvation, hypoxia, oxidative stress, drug treatment or DNA damage (He and Klionsky, 2009). In both cases, autophagy represents a pro-survival mechanism allowing quality control, metabolic reprogramming or cell fitness after a stress (Semenza, 2010; Mehrpour et al., 2010; Codogno and Meijer, 2005; Shannon et al., 2003; Brahimi-Horn and Pouyssegur, 2006). Moreover, evidence that autophagy plays a role in maintaining cancer cell survival in their microenvironment where nutrients and oxygen are reduced or in response to anticancer chemotherapies have been reported (Notte et al., 2013; Checinska and Soengas, 2011; Notte et al., 2011; Morselli et al., 2009; Shen et al., 2012; White, 2012; Song et al., 2009; Zhang et al., 2008).

The second signaling mechanism that could play a role in cancer cell resistance is UPR that is activated by ER (endoplasmic reticulum) stresses. UPR is induced by several perturbations in ER homeostasis (change in cellular energy, redox state or Ca^{2+} homeostasis) leading to the accumulation of mis- or unfolded proteins in the ER compartment. In mammalian cells, UPR is transduced by three ER transmembrane protein sensors namely PERK (protein kinase RNA (PKR)-like ER kinase), IRE1α (inositol-requiring enzyme-1) and ATF6 (activating transcription factor-6) (Ron and Walter, 2007). The ER chaperone GRP78/BIP (78 kDa glucose-regulated protein/immunoglobulin heavy chain-binding protein) binds to the luminal domains of PERK, IRE1α, and ATF6 in unstressed cells to maintain them in an inactive state (Shen et al., 2002; Bertolotti et al., 2000). Unfolded protein load triggers the dissociation of GRP78/BIP from these sensors triggering the UPR activation. PERK then forms homodimers and is activated by trans-autophosphorylation. PERK phosphorylates the alpha-subunit of eIF2 (eukaryotic translation initiation factor-2) leading to translational attenuation of capped mRNA and thus to protein synthesis inhibition to prevent additional accumulation of newly synthesized proteins into the ER. However, PERK signaling also selectively induces the expression of ATF4 (activating transcription factor-4) through the bypass of a micro-ORF upstream of ATF4 open reading frame (Harding et al., 2000). IRE1 contains a serine/threonine protein kinase domain and an endoribonuclease domain within the C-terminal cytosolic region. Activation of IRE1 is driven by its oligomerization and trans-autophosphorylation. Once activated, IRE1 splices an unconventional intron from the XBP1 (X-box binding protein-1) mRNA to generate an active spliced form of XBP1 transcription factor that controls the expression of UPR target genes leading to an adaptive response. Upon ER stress, ATF6 is transported to the Golgi apparatus where it is cleaved generating an active fragment containing a DNA binding domain. Cleaved ATF6 translocate to the nucleus and activates the transcription of UPR target genes (Bravo et al., 2013; Chakrabarti et al., 2011; Walter and Ron, 2011; Urano et al., 2000). The primary function of UPR is thus to reestablish ER homeostasis by lowering protein synthesis and translocation into the ER, by increasing the capacity of the ER to handle unfolded proteins and by the removal of misfolded proteins via the ERAD (ER-associated protein degradation) system (Travers et al., 2000). When the ERAD system is saturated and unable to degrade misfolded or aggregated proteins, UPR can also induce autophagy as an alternative mechanism for protein degradation (Yorimitsu and Klionsky, 2007) PERK, IRE1α, and ATF6 signaling pathways are now known to control autophagy (Deegan et al., 2012; Hoyer-Hansen and Jaattela, 2007; Kouroku et al., 2007; Garcia-Navas et al., 2012). If activation of these pro-survival mechanisms is insufficient to overcome the ER stress, prolonged activation of UPR triggers apoptosis (Vannuvel et al., 2013; Szegezdi et al., 2006, 2009; Heath-Engel et al., 2008). Interestingly, the high proliferative rate of cancer cells generates a stressful hypoxic environment in which UPR is often chronically activated and acts as a pro-survival mechanism (Rouschop et al., 2010; Koumenis, 2006; Bi et al., 2005; Romero-Ramirez et al., 2004; Shajahan et al., 2009). While the role of UPR in chemotherapy resistance has already been demonstrated in several works (Jiang et al., 2008; Feng et al., 2011; Rzymski et al., 2009; Milani et al., 2009; Li and Lee, 2006; Wang et al., 2009; Kumandan et al., 2013; Chen et al., 2011; Mann and Hendershot, 2006), it has never been studied in combination with a hypoxic environment in the resistance against taxol-induced apoptosis. Since UPR is involved in the regulation of autophagy and apoptosis (Kiviluoto et al., 2013), a better understanding of the mechanisms by which UPR controls cell fate decision in these conditions represents a necessary step in the field of anti-cancer therapy (Healy et al., 2009; Schonthal, 2013).

We previously showed that apoptosis is activated in MDA–MB-231 breast cancer cells incubated with taxol (Notte et al., 2013). In these conditions, autophagy is activated much earlier than apoptosis and is a protective mechanism. MDA–MB-231 cells incubated with taxol under hypoxia are more resistant than cells incubated with the anticancer agent alone, because hypoxia stimulates a more effective autophagic flow (Notte et al., 2013). In the present work, we studied whether taxol-induced UPR activation would be an upstream event leading to the activation of autophagy and/or apoptosis. The role of UPR in the hypoxia-induced resistance against taxol-induced cell death and its link with autophagy and apoptosis activation were thus investigated. Results show a specific role for ATF4 in taxol-induced autophagy as a mechanism promoting cancer cell adaptation and survival under hypoxia.

2. Material and methods

2.1. Cell culture and hypoxia incubation

Human breast cancer cells MDA–MB-231 were maintained in culture in 75 cm^2 polystyrene flasks (Costar, Lowell, MA, USA) with 15 ml of Roswell Park Memorial Institute medium (RPMI 1640 Invitrogen, Carlsbad, CA, USA) containing 10% of fetal calf serum (Invitrogen). Human breast cancer cells T47D were maintained in culture in 75 cm^2 polystyrene flasks (Costar, Lowell, MA, USA) with 15 ml of Dulbecco's modified Eagle medium (DMEM, Invitrogen) containing 10% of fetal calf serum (Invitrogen) and 1% glutamine (Sigma, St. Louis, USA). Both cell types were incubated under an atmosphere containing 5% CO_2.

For hypoxia experiments (1% O_2), cells were incubated in serum-free CO_2-independent medium (Invitrogen) supplemented with 1 mM L-glutamine (Sigma) with or without 50 μM paclitaxel (Molecular Probes, Carlsbad, CA, USA) at 50 μM. Normoxic control cells were incubated in the same conditions but in normal atmosphere (20% O_2).

2.2. Plasmid transfection and dual-luciferase reporter assay

Cells were seeded in 12-well culture plates (100,000 cells/well) 24 h before being transfected with 0.9 μg/well of the plasmid containing the firefly luciferase gene and 0.1 μg/well of the plasmid containing the renilla luciferase gene (for normalization of transfection efficiency) using the lipofectamine transfection reagent (from Invitrogen). ATF6 activity was measured using a luciferase reporter

gene construct in which the firefly luciferase gene is driven by a promoter containing five copies of the ATF6/XBP1 binding element (Zeng et al., 2004). ATF6 reporter plasmid was also used to confirm ATF6 invalidation. In these experimental conditions, cells were co-transfected with 50 nM of ATF6 siRNA. Transfection medium was removed and replaced by complete medium for 24 h. Cells were then incubated as previously described (Notte et al., 2013). After incubation, the luciferase reporter assay was performed using the dual-luciferase reporter assay system kit (E1910, from Promega) according to the manufacturer's instructions.

2.3. Caspase 3 activity assay

The fluorogenic substrate Ac-DEVD-AFC was used to measure caspase 3 activity according to Lozano et al. (2001) Cell extracts were prepared as described by Wellington et al. (1998). Cells were seeded in 25 cm^2 polystyrene flasks (Costar) (800,000 cells/well) 24 h before the incubation. After the incubation, the medium was recovered and centrifuged at 1200 rpm for 5 min. Cells that were still attached to the well were scrapped in 500 μl cold PBS and recovered into a microtube. Pelleted detached cells were resuspended in 100 μl PBS at 4 °C and pooled with respective attached cell sample to the microtube. The samples were centrifuged at 1200 rpm for 5 min. at 4 °C and the pellet resuspended in 50 μl of lysis buffer (10 mM Hepes/KOH, pH 7.0, 10% sucrose, 2 mM EDTA, 0.1% CHAPS, 5 mM dithiothreitol, and 10 μg/ml aprotinin). After incubation on a rotating wheel for 15 min at 4 °C, the lysates were centrifuged at 13,000 rpm for 5 min at 4 °C and the supernatants were recovered for the assay.

The protein concentration was determined (Pierce 660, Thermo Scientific) and 10 μg of proteins completed to a volume of 75 μl with lysis buffer were mixed with 1 μl Ac-DEVD-AFC (BD Pharmingen, 556574) and 75 μl reaction buffer (40 mM PIPES, pH 7.2, 200 mM NaCl, 2 mM EDTA, 0.2% CHAPS, 0.10% sucrose, and 10 mM dithiothreitol). The reaction was allowed to take place for 1 h at 37 °C and the fluorescence generated by the release of the fluorogenic group AFC after cleavage by caspase 3/7 was measured in a spectrophotometrer (excitation λ: 400 nm and emission λ: 505 nm).

2.4. LDH release assay

LDH release assay has been described in Notte et al. (2013).

2.5. Western blotting

Procedure for Western blotting analyses has been described in Notte et al. (2013). Primary antibodies used are referenced in supplementary Table 1.

2.6. RT-qPCR

Procedure for RT-qPCR has been described in Notte et al. (2013). Forward and reverse primers for RPL13A, PERK, IRE1α, and ATF6 were designed using the Primer Express 1.5 software (Applied Biosystem).

2.7. siRNA transfection

Silencing of PERK, IRE1α, ATF6, and ATF4 expression was achieved using ON-TARGET plus SMARTpool human PERK (L004883, from Dharmacon), ON-TARGET plus SMARTpool human ERN1 (IRE1α) (L004951, from Dharmacon), ON-TARGET plus SMARTpool human ATF6 (L009917, from Dharmacon), ON-TARGET plus SMARTpool human CREB2 (ATF4) (L005225, from Dharmacon), ON-TARGET plus SMARTpool human GCN2 (L005314, from Dharmacon), ON-TARGET plus SMARTpool human HRI (L005007, from Dharmacon),and ON-TARGET plus SMARTpool human PKR (L003527, from Dharmacon). Risc-ree control siRNA purchased from Dharmacon was used as a negative control. For siRNA experiments, 8×10^5 cells were seeded in 25 cm^2 polystyrene flasks (Costar) with 4 ml of RPMI 1640 medium (RPMI) containing 10% of fetal calf serum and incubated for 24 h under an atmosphere containing 5% CO_2. Cells were then transfected for 24 h under standard culture conditions with 50 nM siRNA when transfected alone, or 25 nM of each siRNA when co-transfected using the DharmaFECT 1 (Dharmacon) transfection reagent according to the manufacturer's instructions. The transfection media were removed and replaced by culture media for 24 h. Cells were then incubated as previously described (Notte et al., 2013).

2.8. Kaplan–Meier curves

An Affymetrix dataset containing gene expression data from 249 breast cancer patients for whom complete demographic, histological grade, stage, differentiation information are available, was used for survival studies (downloaded from GEO, GSE4922, Uppsala cohort). Procedures of RNA extraction and hybridization are described in Ivshina et al. (2006). Raw data in CEL files are publicly available and were processed according to the method defined by Pierre et al. (2010), by using alternative CDFs from AffyProbeMiner and GCRMA for normalization and summarization of downloaded data in the *R* statistical environment. Kaplan–Meier curves were drawn in the R statistical environment for each subgroup. 249 patients were separated in two equal subgroups ($n = 124/n = 125$) according to the expression of one gene. These subgroups were then subdivided when combinations of several gene expressions were studied.

2.9. Statistical analysis

SigmaStat software (Jandle Scientific, Germany) was used for the statistical analysis. Data are presented as means ± standard deviation (SD) and were evaluated by one-way or two-way ANOVA, using the Holm–Sidak method.

3. Results

3.1. PERK, IRE1α, and ATF6 pathways are activated in breast cancer cell lines during taxol exposure under normoxia and hypoxia

To examine whether taxol induces an ER stress in breast cancer cells, activation of the three branches of the UPR was studied. MDA–MB-231 cells were incubated under normoxia or hypoxia with or without 50 μM taxol. Phosphorylation of eIF2α and IRE1α was assessed, by Western analysis, after 2, 4, 8, 16, and 24 h of incubation (Fig. 1A). The results showed that taxol induced IRE1α phosphorylation already after 4 h of incubation under normoxia or hypoxia. The level of phosphorylation increased with time and became statistically significant at 16 h. Moreover, taxol also induced the phosphorylation of eIF2α: a significant increase of respectively 3.5 and 5 fold was observed after 2 and 4 h of incubation. Hypoxia alone induced eIF2α phosphorylation as observed after 24 h of incubation. For long incubation times, taxol-induced eIF2α phosphorylation decreased. Hypoxia did not influence eIF2α and IRE1α phosphorylation induced by taxol.

In order to confirm these results, we used another breast cancer cell line, T47D cells. This cell line is also protected against taxol-induced apoptosis and cell death by hypoxia as evidenced by a reduced activation of caspase 3 and PARP cleavage as well as a

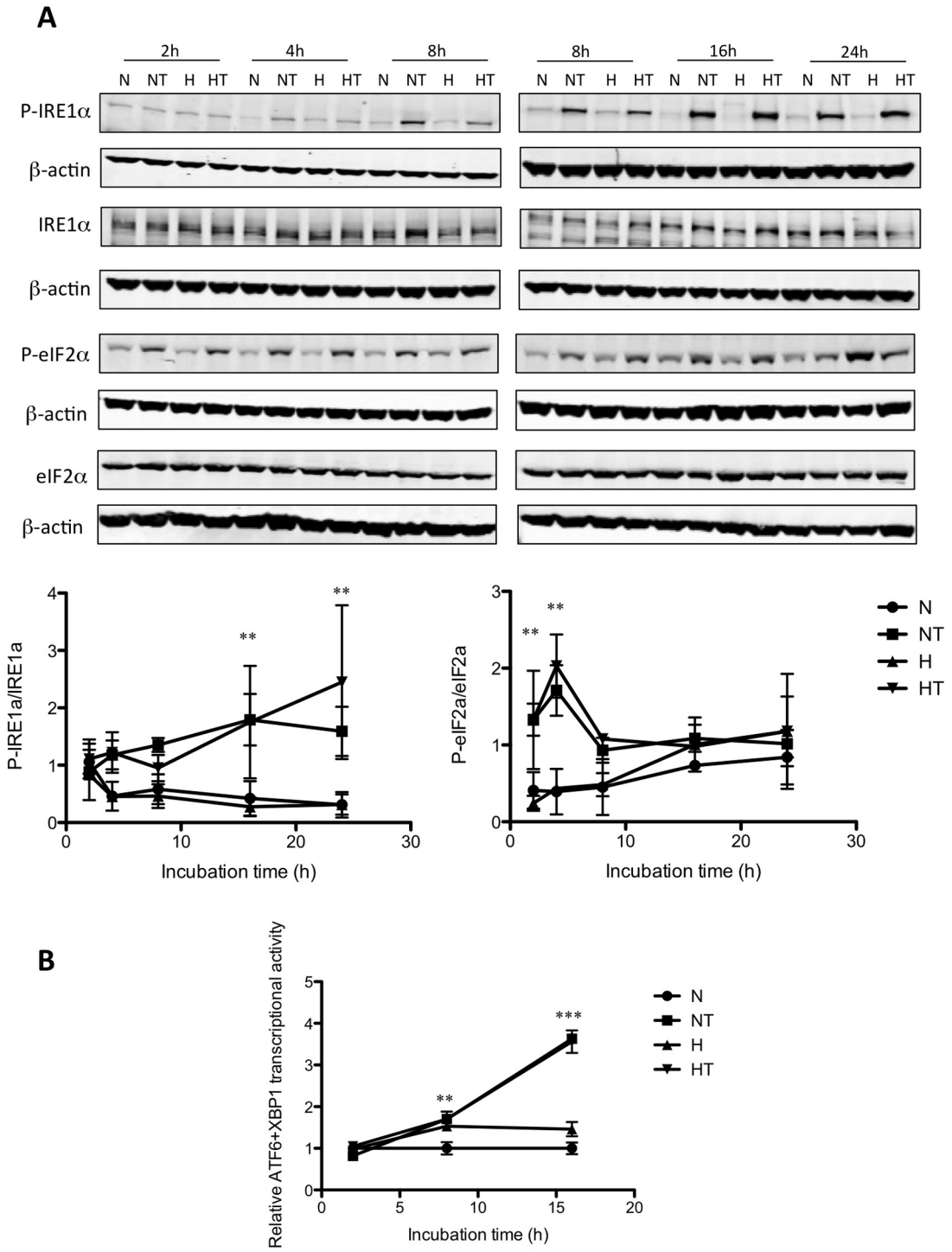

Fig. 1. PERK, IRE1α, and ATF6 pathways are activated after taxol exposure under normoxia and hypoxia in MDA-MB-2331 cells. MDA–MB-231 cells were incubated under normoxia (N) or hypoxia (H) without or with taxol (T) at 50 μM. **A.** After 2, 4, 8, 16, and 24 h of incubation, the abundance of phospho-eIF2α, eIF2α, phospho-IRE1α, and IRE1α was assessed in total cell extracts by western blotting analysis, using specific antibodies. β-actin was used to assess the total amount of proteins loaded on the gel. Uncropped western blots are presented in the supplementary figure 6. The graphs below represent the quantification of phospho-IRE1α abundance normalized to total IRE1α abundance and of phospho-eIF2α abundance normalized to eIF2α abundance for three independent experiments. The results are presented as means ± 1 S.D. ($n = 3$). ** $p < 0.01$ vs time matched control cells, using ANOVA 2 and Sidak–Holm test as post hoc test. **B.** Cells were co-transfected during 4 h with firefly-luciferase reporter ATF6/XBP1 plasmid and renilla luciferase reporter plasmid 24 h before incubation. After 2, 8, and 16 h of incubation, ATF6/XBP1 activity was assayed using the dual luciferase reporter assay. Data are expressed in relative ATF6 transcriptional activity normalized to the control cells (N) and presented as means ± 1 S.D. ($n = 3$). ** $p < 0.01$; *** $p < 0.001$ vs time matched control cells, using ANOVA 2 and Sidak–Holm test as post hoc test.

lower LDH release (supplementary Figure 1). Similar results on the phosphorylation of eIF2α and IRE1α induced by taxol were obtained for T47D cells as shown for 8 and 16 h of incubation (Fig. 2A). Next, ATF6 activity was measured after 2, 8, and 16 h of incubation in cells transiently transfected with an ATF6/XBP1-specific luciferase reporter construct in which the firefly luciferase reporter gene is driven by a promoter containing five copies of the ATF6/XBP1 binding element (Zeng et al., 2004) (Fig. 1B).

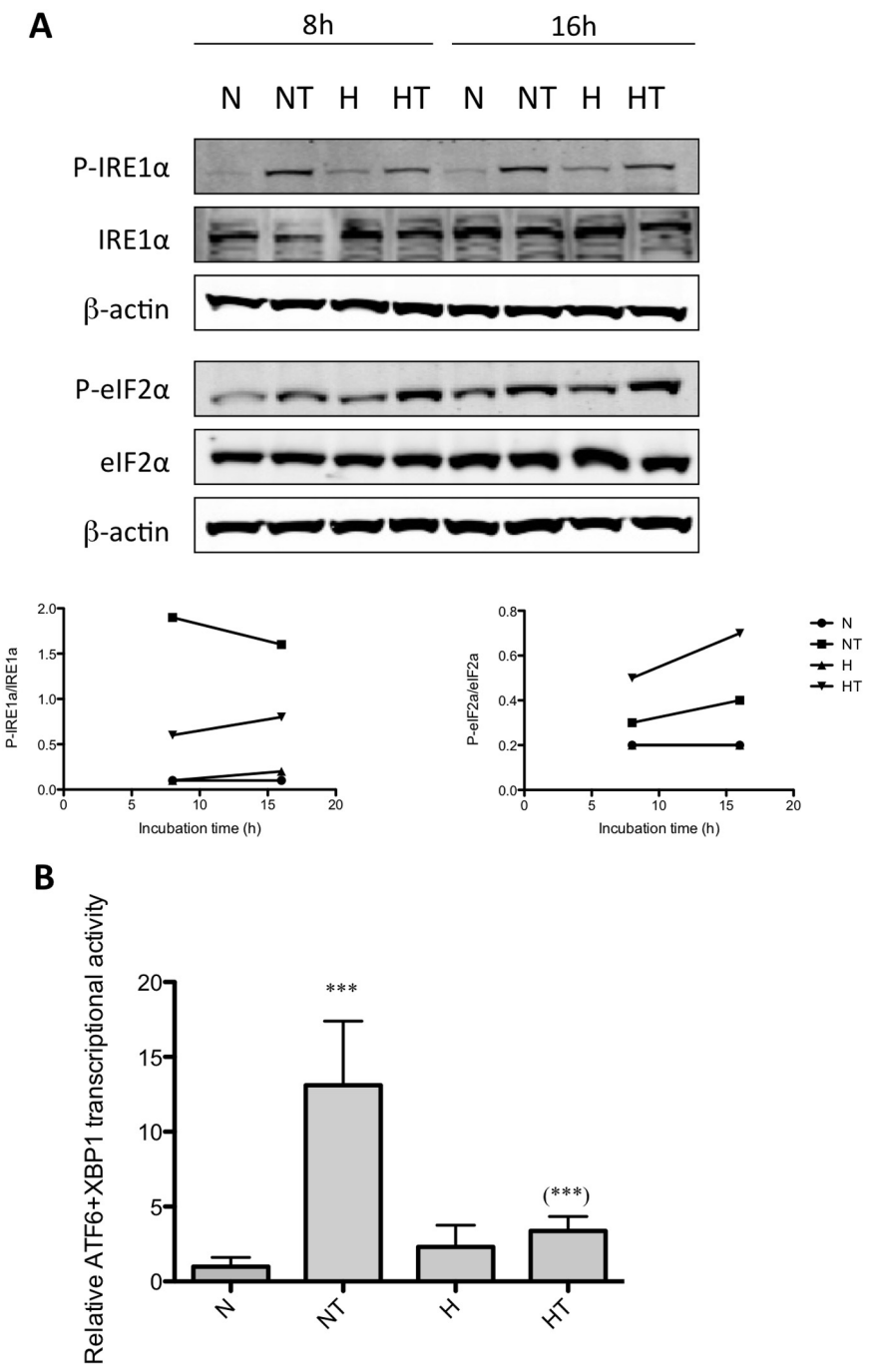

Fig. 2. PERK, IRE1α, and ATF6 pathways are activated after taxol exposure under normoxia and hypoxia in T47D cells.
T47D cells were incubated under normoxia (N) or hypoxia (H) without or with taxol (T) at 50 μM.A. After 8 and 16 h of incubation, the abundance of phospho-eIF2α, eIF2α, phospho-IRE1α, and IRE1α was assessed in total cell extracts by western blotting analysis, using specific antibodies. β-actin was used to assess the total amount of proteins loaded on the gel. The graphs below represent the quantification of phospho-IRE1α abundance normalized to total IRE1α abundance and of phospho-eIF2α abundance normalized to eIF2α abundance. Uncropped western blots are presented in the supplementary figure 6. **B.** Cells were co-transfected during 4 h with firefly-luciferase reporter ATF6 plasmid and renilla-luciferase reporter plasmid 24 h before incubation. After 16 h of incubation, ATF6 activity was assayed using the dual luciferase reporter assay. Data are expressed in relative ATF6 transcriptional activity normalized to the control cells (N) and presented as means ± 1 S.D. (two independent experiments with $n = 4$). *** $p < 0.001$ vs normoxic control cells; *** $p < 0.001$ vs NT using ANOVA 2 and Sidak–Holm test as post hoc test.

ATF6 was activated in MDA–MB-231 cells incubated for 8 h with taxol but no difference could be observed between cells incubated with taxol under normoxia or hypoxia. Taxol similarly increased ATF6/XBP1 transcriptional activity in T47D cells but, in this cell line, hypoxia inhibited the taxol-induced ATF6/XBP1 activation (Fig. 2B).

3.2. Activation of UPR is neither involved in apoptosis nor in autophagy induced by taxol

Recent studies have shown that UPR activation leads to the induction of either autophagy or apoptosis (Deegan et al., 2012; Rasheva and Domingos, 2009). Several arguments support the role

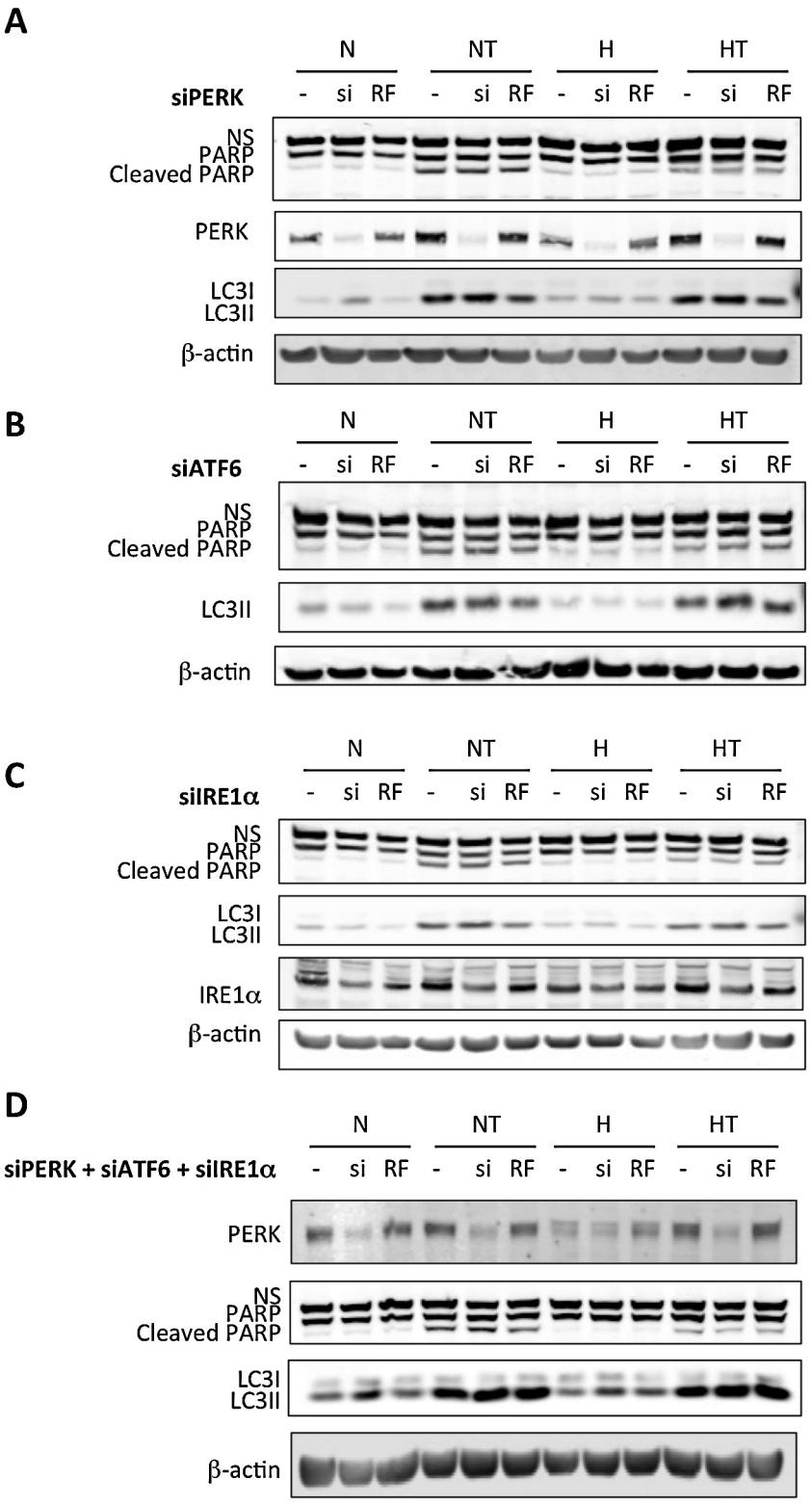

Fig. 3. Activation of UPR is neither involved in taxol-induced apoptosis nor in autophagy. MDA–MB-231 cells were untransfected (−) or transfected with 50 nM of PERK (**A**), ATF6 (**B**), or IRE1α (**C**) siRNA (si) or negative control Risc Free siRNA (RF) for 24 h (**D**). MDA–MB-231 cells were untransfected (−) or co-transfected with 25 nM of PERK, ATF6, and IRE1α siRNA (si) or 75 nM of negative control Risc-free siRNA (RF) for 24 h. The transfection media were removed and replaced by culture media for 24 h. Cells were then incubated under normoxia (N) or hypoxia (H) for 16 h, without or with taxol (T) at 50 μM. PARP cleavage, LC3II, PERK, and IRE1α abundance was detected in total cell extracts by western blotting analysis, using specific antibodies. β-actin was used to assess the total amount of proteins loaded on the gel. Uncropped western blots are presented in the supplementary figure 6. NS: nonspecific band.

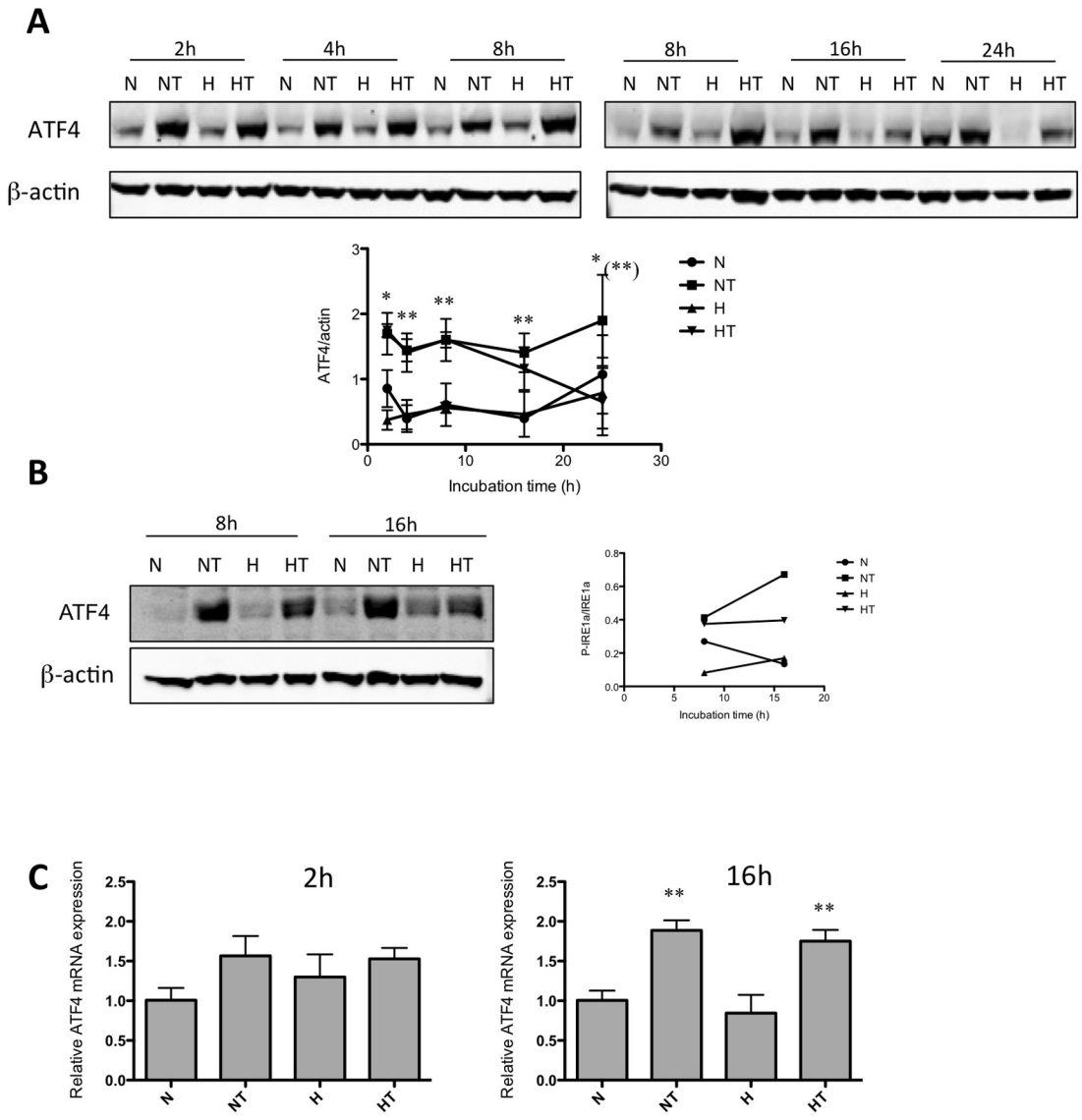

Fig. 4. ATF4 pathway is activated after taxol exposure. MDA–MB-231 (**A, C**) and T47D (**B**) cells were incubated under normoxia (N) or hypoxia (H) without or with taxol (T) at 50 μM for different incubation times. **A, B**. After the incubation, the abundance of ATF4 was assessed in total cell extracts by Western blotting analysis, using specific antibodies. β-actin was used to assess the total amount of proteins loaded on the gel. The graphs below represent the quantification of ATF4 abundance normalized to ß-actin abundance. Uncropped western blots are presented in the supplementary figure 6. The graphs below represent the quantification of phospho-IRE1α abundance normalized to total IRE1α abundance for three independent experiments. The results are presented as means ± 1 S.D. ($n = 3$). * $p < 0.05$; ** $p < 0.01$ vs time matched control cells; ** $p < 0.01$ HT vs NT, using ANOVA 2 and Sidak–Holm test as post hoc test. **C.** After 2 or 16 h of incubation, total RNA was extracted, mRNAs were retrotranscribed and ATF4 mRNA levels analyzed by RT-qPCR. The results are presented as means ± 1 S.D. ($n = 3$). ** $p < 0.01$ vs time matched control cells using ANOVA 1 and Sidak–Holm test as post hoc test.

of UPR in these biological processes. PERK induces eIF2α phosphorylation leading to ATF4 activation that can induce Atg12 and LC3 expression (Kouroku et al., 2007; Rouschop et al., 2010). Moreover, ATF4 induces CHOP10 expression and activation, a transcription factor that controls the expression of TRB3 (Ohoka et al., 2005), a protein from the Bcl_2 family (McCullough et al., 2001) and Atg5 (Rouschop et al., 2010), and could thus act as a pro-apoptotic or a pro-autophagic transcription factor. In addition, ATF6 and XBP1 are also known to enhance CHOP10 expression (Oyadomari and Mori, 2004). IRE1α may also regulate autophagy and apoptosis by activating the JNK signaling pathway (Urano et al., 2000; Nishitoh et al., 2002; Ogata et al., 2006).

To investigate whether one of these pathways regulates taxol-induced autophagy or apoptosis, PERK, ATF6, and IRE1α expression was silenced in MDA–MB-231 cells transfected with PERK (Fig. 3A), ATF6 (Fig. 3B), or IRE1α (Fig. 3C) siRNAs independently or in combination (Fig. 3D). The efficiency of invalidation of the target proteins was analyzed by western blotting (for PERK and IRE1α, Fig. 3) as well as by RT-qPCR (for PERK, IRE1α, and ATF6) or by measuring transcriptional activity (for ATF6) (see supplementary figures 2 and 3). Results showed that neither independent nor combined knock down of the three ER-stress sensors did modulate the abundance of taxol-induced autophagy or apoptosis markers. Indeed, no difference in the abundance of LC3II or in PARP cleavage was observed between cells transfected with the specific siRNAs and cells transfected with control siRNA (Fig. 3).

3.3. *ATF4 is involved in taxol-induced activation of autophagy*

ATF4 is another player of UPR, which is downstream of PERK. It is known to be induced by tumor microenvironment factors

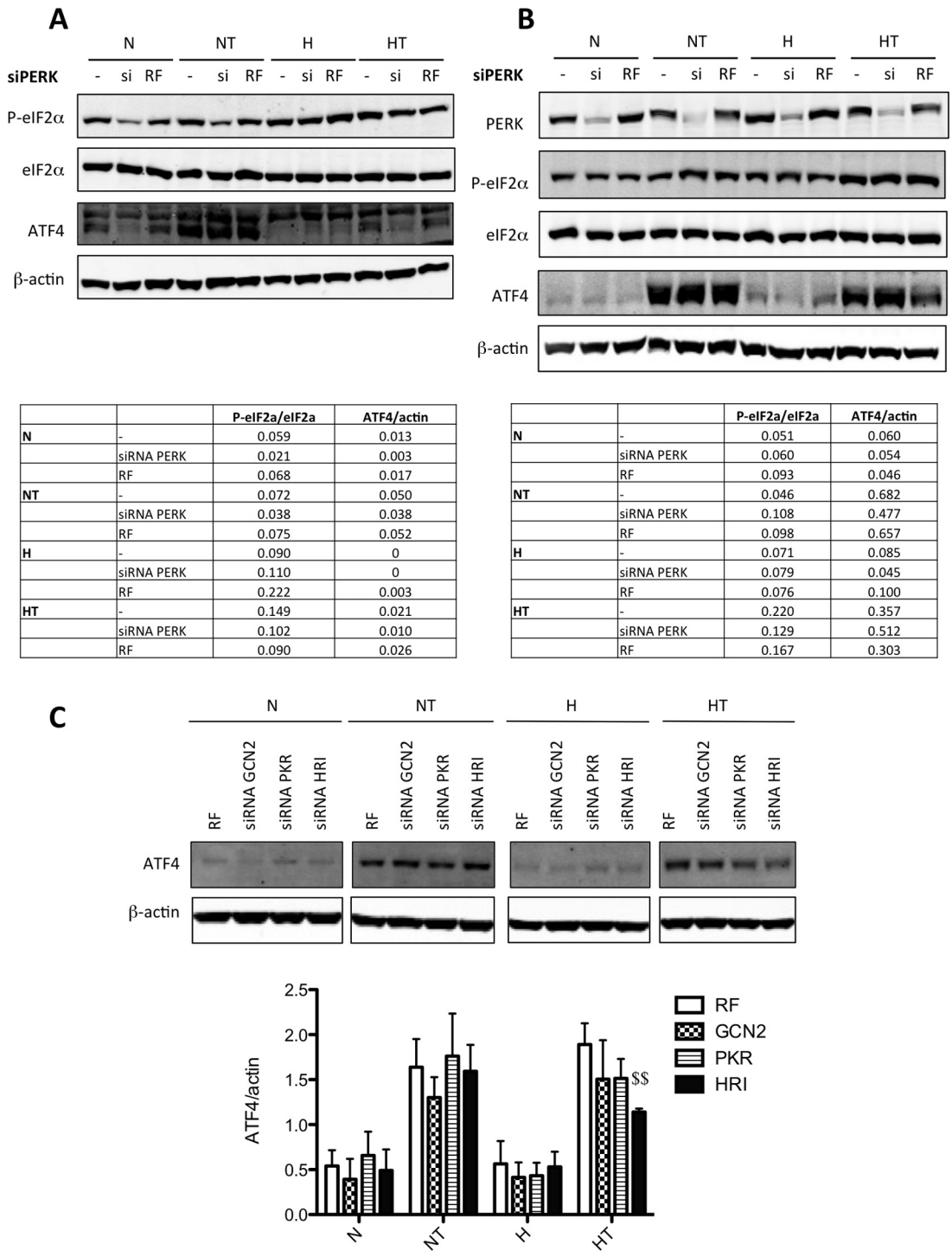

		P-eIF2a/eIF2a	ATF4/actin
N	-	0.059	0.013
	siRNA PERK	0.021	0.003
	RF	0.068	0.017
NT	-	0.072	0.050
	siRNA PERK	0.038	0.038
	RF	0.075	0.052
H	-	0.090	0
	siRNA PERK	0.110	0
	RF	0.222	0.003
HT	-	0.149	0.021
	siRNA PERK	0.102	0.010
	RF	0.090	0.026

		P-eIF2a/eIF2a	ATF4/actin
N	-	0.051	0.060
	siRNA PERK	0.060	0.054
	RF	0.093	0.046
NT	-	0.046	0.682
	siRNA PERK	0.108	0.477
	RF	0.098	0.657
H	-	0.071	0.085
	siRNA PERK	0.079	0.045
	RF	0.076	0.100
HT	-	0.220	0.357
	siRNA PERK	0.129	0.512
	RF	0.167	0.303

Fig. 5. eiF2α and ATF4 pathways are activated after taxol exposure independently of PERK. MDA–MB-231 (**A, C**) or T47D (**B**) cells were untransfected (−) or transfected with 50 nM of PERK siRNA (si) or negative control Risc-free siRNA (RF) for 24 h. The transfection media were removed and replaced by culture media for 24 h. Cells were then incubated under normoxia (N) or hypoxia (H) for 16 h, without or with taxol (T) at 50 μM. Phospho-eIF2α, eIF2α, ATF4 and PERK abundance was assessed in total cell extracts by Western blotting analysis, using specific antibodies. β-actin was used to assess the total amount of proteins loaded on the gel. **A, B**. The tables below represent the quantification of phospho-eIF2α abundance normalized to eIF2α abundance and of ATF4 normalized to ß-actin abundance. Uncropped western blots are presented in the supplementary figure 6. **C.** The graphs below represent the quantification of ATF4 abundance normalized to ß-actin abundance for three independent experiments. The results are presented as means ± 1 S.D. ($n = 3$). $^{\$\$}$ $p < 0.01$ vs corresponding RF transfected cells, using ANOVA 2 and Sidak–Holm test as post hoc test.

such as hypoxia (Koumenis, 2006) and to play a role in cancer progression (Ameri and Harris, 2008) as well as in autophagy regulation (Rzymski et al., 2009; Milani et al., 2009). Moreover, other kinases than PERK are able to phosphorylate eIF2α leading to ATF4 activation (Donnelly et al., 2013). These kinases, GCN2 (general control non-derepressible-2), HRI (heme-regulated inhibitor), and PKR (double stranded RNA-dependent protein kinase), are activated after amino acid starvation (Harding et al., 2000), oxidative stress/proteasome degradation inhibition (Lu et al., 2001; Yerlikaya et al., 2008), and viral infection (Kiviluoto et al., 2013) respectively. They belong to the family of kinases that control the integrated stress response (ISR).

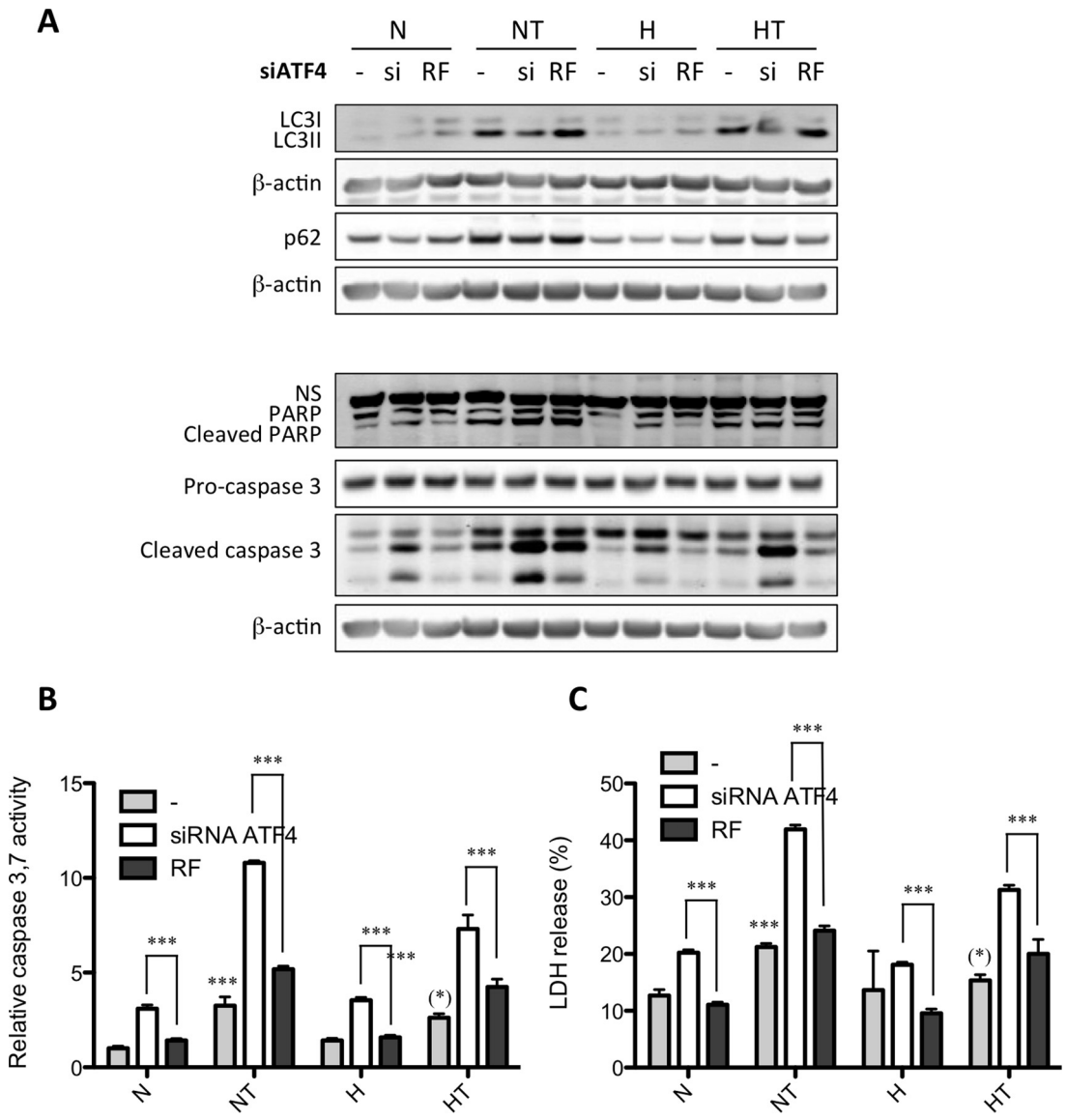

Fig. 6. ATF4 is involved in autophagy activation after taxol exposure in MDA–MB-231 cells. (**A, B, C**) MDA–MB-231 cells were untransfected (−) or transfected with ATF4 siRNA (si) or negative control Risc Free siRNA (RF) at 50 nM for 24 h. The transfection media were removed and replaced by culture media for 24 h. Cells were then incubated under normoxia (N) or hypoxia (H) for 16 h, without or with taxol (T) at 50 μM. A. The abundance of PARP, cleaved PARP, cleaved caspase 3, LC3, and p62 was detected in total cell extracts by Western blotting analysis, using specific antibodies. β-actin was used to assess the total amount of proteins loaded on the gel. Uncropped western blots are presented in the supplementary figure 6. NS: nonspecific band. B. Caspase 3 and 7 activity was assayed by measuring fluorescence intensity associated with free AFC released by the cleavage of the flouorogenic Ac-DEVD-AFC substrate by caspase 3 and 7. Results are expressed in relative caspase 3/7 activity normalized to fluorescence intensity of the untransfected control cells and presented as means ± 1 S.D. ($n = 3$). C. After 40 h of incubation, LDH release was assessed. Results are expressed in percentages of cytotoxicity as means ± 1 S.D. ($n = 3$). *** $p < 0.001$ vs normoxic control cells; (*) $p < 0.05$ vs NT; *** $p < 0.001$ vs corresponding RF-transfected cells using ANOVA 2 and Sidak–Holm test as post hoc test.

ATF4 activation was thus investigated in MDA–MB-231 (Fig. 4A) and in T47D (Fig. 4B) cells exposed to taxol under normoxia or hypoxia. Results showed that ATF4 protein level was increased in cells incubated in the presence of taxol. Hypoxia seemed to decrease the taxol-induced increase in ATF4 protein level at long incubation time (24 h). It has to be noted that ATF4 was observed as a doublet on western blot analysis. This has already been observed in several other studies. (Pan et al., 2013; Yu et al., 2013) This may be due to phosphorylation, as demonstrated in Lassot et al. (2001). Since there is a strong decrease in the intensity of these bands in lanes corresponding to protein extracts of cells transfected with ATF4 siRNA (Fig. 7), we concluded that the detection was specific for this protein.

In order to analyze the mechanism by which ATF4 protein level was increased, ATF4 mRNA level has been analyzed. The results showed that taxol significantly increased by 2-fold ATF4 mRNA level after 16 h of incubation (Fig. 4C). Hypoxia alone has no effect and did not affect the effect of taxol. It must be noted that ATF4 protein level was upregulated by 2fold already after 2 h of incubation in the presence of taxol (Fig. 4A). While it does not exclude that an increase in ATF4 mRNA was responsible for the upregulation of the protein level at longer incubation times, the increase observed at 2 h is more probably due to post-translational regulation. Indeed, the mRNA level of ATF4 was also measured after 2 h incubation in the presence of taxol and there was no significant change induced by taxol (Fig. 4C).

Since we showed that PERK is activated by taxol, we investigated whether this kinase is the enzyme that could be responsible for ATF4 accumulation in both cell breast cancer cell lines. For that, PERK was thus invalidated using siRNA but no effect was

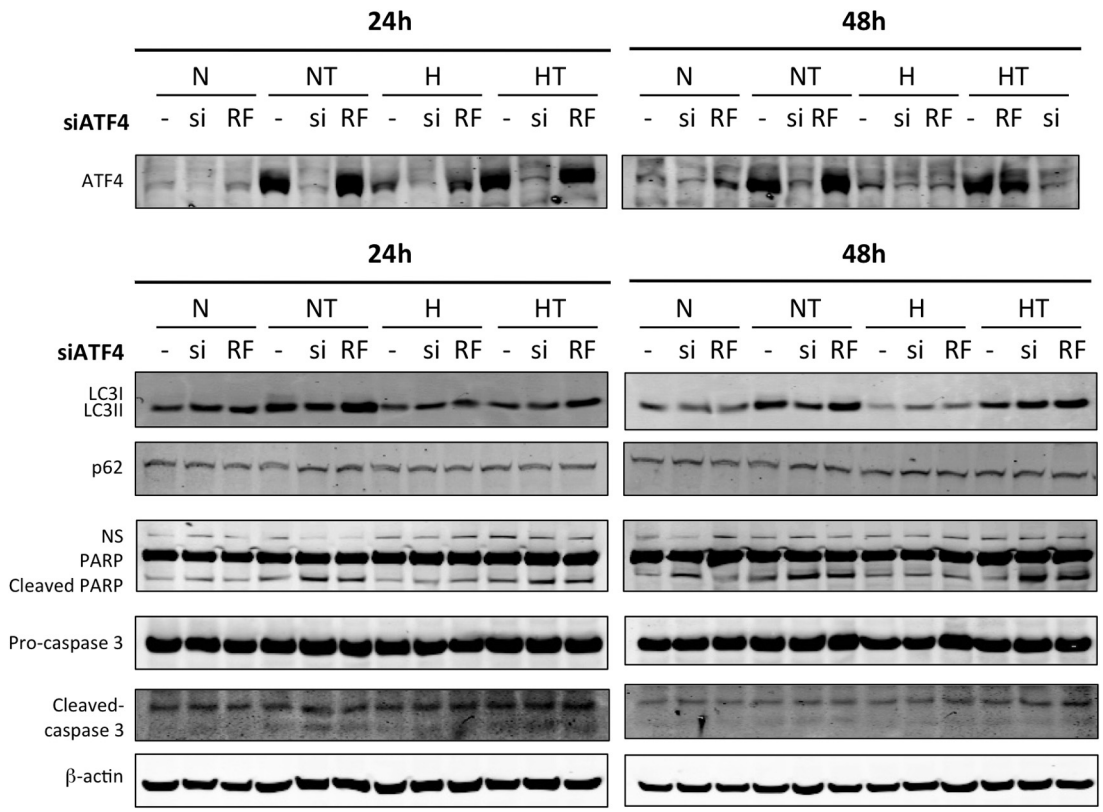

Fig. 7. ATF4 is involved in autophagy activation after taxol exposure in T47D cells. T47D cells were untransfected (−) or transfected with ATF4 siRNA (si) or negative control Risc Free siRNA (RF) at 50 nM for 24 h. The transfection media were removed and replaced by culture media for 24 h. Cells were then incubated under normoxia (N) or hypoxia (H) for 16 h, without or with taxol (T) at 50 μM. The abundance of ATF4, PARP, cleaved PARP, p62, cleaved caspase 3 and LC3 was detected in total cell extracts by Western blotting analysis, using specific antibodies. β-actin was used to assess the total amount of proteins loaded on the gel. Uncropped western blots are presented in the supplementary Fig. 6. NS: nonspecific band.

observed on eiF2α phosphorylation in response to taxol, except in MDA–MB-231 cells under normoxia (Fig. 4C and 4D). Furthermore, the taxol-induced increase in ATF4 protein level was not modified in MDA–MB-231 cells maintained in normoxia (Fig. 4C) nor in T47D cells maintained in normoxia or exposed to hypoxia (Fig. 4D). These results suggest that ATF4 accumulation results from the activation of the ISR when breast cancer cells are exposed to taxol.

Inorder to verify this hypothesis, each of the three kinases from the IRS has been silenced by siRNA. The controls for silencing are presented in the supplementary Fig. 4. Three independent experiments were performed. The results suggest that HRI is the kinase involved in this effect since there was a significant decrease in the taxol-induced increase in ATF4 protein level when this kinase was silenced, on the contrary to the two other kinases, GCN2 and PKR (Fig. 5C). These results suggest that IRS may be responsible for the taxol-induced increase in ATF4 protein level.

Since ATF4 is activated by an UPR-independent signaling pathway, the role of ATF4 in the adaptation to hypoxia or in taxol-induced autophagy was investigated. MDA–MB-231 cells were transfected with ATF4 siRNA or Risc-free siRNA as a negative control. It resulted in ATF4 mRNA silencing to a level lower than 5% (supplementary Fig. 5A). The effects of ATF4 silencing on autophagy or apoptosis were then studied by measuring the abundance of LC3II, cleaved PARP, and cleaved caspase 3 by western blotting (Fig. 6A) as well as by measuring caspase 3/7 activity (Fig. 6B). In addition, overall cytotoxicity was assessed by a LDH release assay (Fig. 6C). In response to ATF4 silencing, taxol-induced LC3II conversion was decreased both under normoxia and hypoxia. PARP and caspase 3 cleavage as well as caspase 3/7 activity and cytotoxicity were significantly increased by ATF4 silencing in cells incubated with or without taxol, under normoxia or hypoxia. ATF4 invalidation also reduced the upregulation of LC3 mRNA level induced by taxol (data not shown). In order to confirm these results, the effect of ATF4 invalidation was also studied in T47D (Fig. 7). Silencing reached more that 90% at the mRNA level (supplementary Fig. 5B). Longer incubation times were used since taxol at 50 μM is less toxic on T47D cells when compared with MDA–MB-231 cells. Results showed that ATF4 silencing decreased the taxol-induced LC3I to LC3II conversion, while it increased taxol-induced PARP and caspase 3 cleavage, as observed for MDA–MB-231 cells. All together, these results suggest that ATF4 not only plays a role in the survival of breast cancer cells under basal conditions but is also involved in the resistance against taxol-induced cell death in part by promoting autophagy.

3.4. ATF4 expression is associated with a poor prognosis in human breast cancer

Finally, we wanted to determine whether ATF4 expression combined to hypoxia could be of clinical interest for breast cancer treatment or prognosis because an increase in ATF4 expression and the presence of hypoxic areas are often associated with tumor development (Koumenis, 2006; Ye and Koumenis, 2009; Ameri et al., 2004). We thus analyzed gene expression data of a public Affymetrix dataset (GSE4922) involving 249 patients (from the Uppsala cohort) with invasive breast tumors. In order to determine whether ATF4 expression could be used as a prognosis biomarker, survival analyses using the Kaplan–Meier method were performed. The cohort of patients was divided into two groups, with one showing high expression and the second one low expression of ATF4, and/or ADM (adrenomedullin, chosen as a hypoxic marker (Winter et al., 2007)). The relapse-free survival probability for patients with

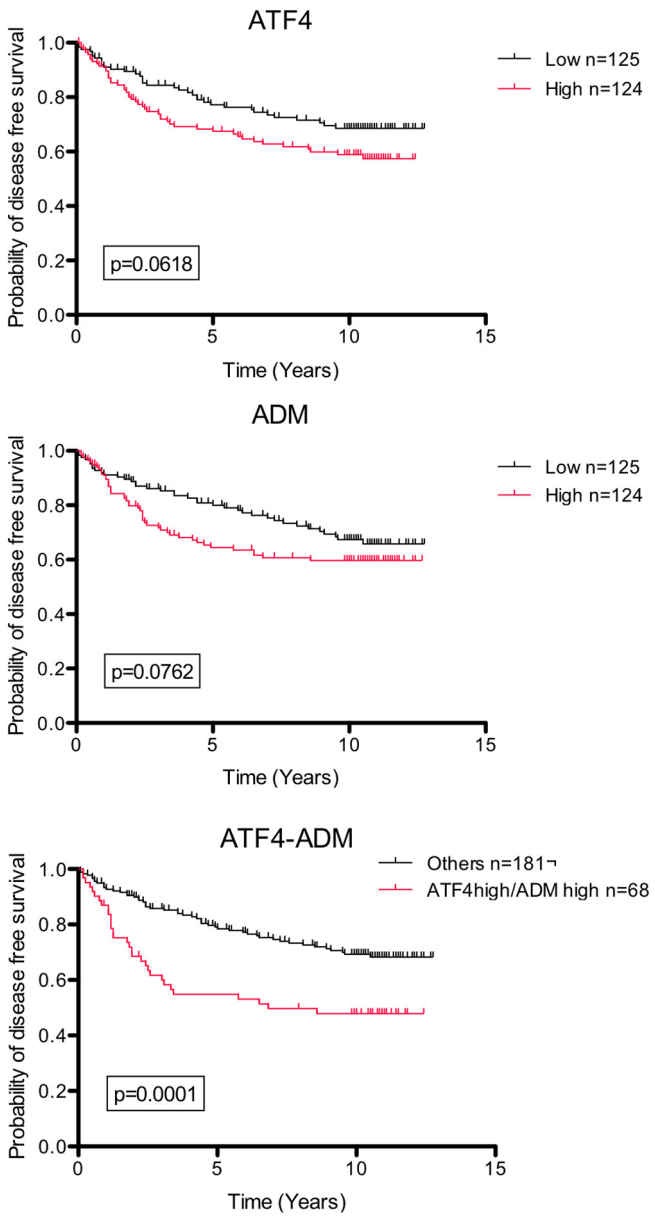

Fig. 8. ATF4 expression in hypoxic breast cancer is a marker of poor prognostic. Public Affymetrix array data of 249 breast cancer patients (GSE4922, Uppsala cohort) for whom cancer specific survival time is known were analyzed. Patients were stratified into two subgroups according to the median value and Kaplan–Meier plots were drawn. Graphs represent the relapse-free survival probability for patients who display high expression versus low expression of ATF4 and/or ADM. Gehan–Breslow–Wilcoxon tests were used for statistical analysis.

low or high gene expression was compared (Fig. 8). Results showed that a high ATF4 expression is associated with a decrease in the probability of survival in patients with breast tumors. ADM, by its own mRNA expression, does seem to influence the survival probability of patients, but this did not reach statistical significance. Patients were then subdivided as a function of the expression of these two genes taken simultaneously. We paralleled the probability of cancer survival between patients displaying a simultaneous high expression of ATF4/ADM vs. all other patients. Patients with a $ATF4^{high}/ADM^{high}$ phenotype had a significantly lower survival ($p < 0.0001$). ATF4 expression is thus a biomarker for a poor prognosis for breast cancer. This prognosis is even worse when ATF4 expression is associated with a hypoxic signature.

4. Discussion

The improvement of chemotherapy is still a big challenge as the number of patients with cancer increases and chemotherapy resistance and relapse are common. In this study, we sought to unravel some mechanisms involved in the resistance of cancer cells against chemotherapy when proliferating in a hypoxic microenvironment. MDA–MB-231 and T47D breast cancer cells were used and incubated with taxol under normoxia or hypoxia. In a previous work, we showed that one mechanism promoting resistance against taxol-induced cell death is the activation of autophagy during taxol exposure. Indeed, hypoxia increases autophagy activation and effectiveness, when compared with normoxia, in cells incubated with taxol (Notte et al., 2013). In this work, the role of UPR and ATF4 was investigated. Taxol induced ER stress as shown by a rapid eIF2α and IRE1α phosphorylation (respectively after 2 and 4 h of incubation) and a later activation of ATF6 (after 8 h of incubation). Hypoxia had no effect on the taxol-induced UPR. Hypoxia alone was also able to induce eIF2α phosphorylation after 24 h of incubation.

Since taxol exposure induced UPR, we decided to investigate whether this activation could be involved in autophagy initiation or in apoptosis activation triggered by taxol exposure. Liao et al. showed that taxol induces ER stress, UPR activation, and apoptosis in U937 cells by an early release of Ca^{2+} and the late amplification of mitochondria-mediated apoptotic signals (Liao et al., 2008). However, they did not study the role of PERK, IRE1α, and ATF6 signaling in apoptosis activation by taxol. The three ER stress sensors were thus silenced, either independently or simultaneously using siRNAs and the effects of UPR inhibition on autophagy and apoptosis were studied. No link between PERK, IRE1α, or ATF6 activation and autophagy or apoptosis regulation could be highlighted.

Next, the involvement of ATF4 in taxol-induced autophagy and apoptosis was investigated. We showed that the transcription factor ATF4 promotes cancer cell survival under basal conditions and during taxol exposure. Indeed, inhibition of ATF4 expression using ATF4 siRNAs resulted in an increase in apoptosis activation and cell death. The protective role of ATF4 after taxol exposure could be due to its capacity to regulate autophagy. Indeed, ATF4 inhibition also led to a decrease in taxol-induced LC3II accumulation. In this study, the decrease in LC3II accumulation can be associated with a decrease in autophagy flow. Furthermore, we showed that ATF4 invalidation decrease LC3b mRNA expression.

In a previous study (Notte et al., 2013), we showed that taxol induced autophagy activation already after 2 h of incubation both under normoxia and hypoxia. Autophagy activation after taxol exposure was shown to be a protective mechanism against taxol-induced cell death both under normoxia and hypoxia. However, at longer incubation time, the autophagic process reached a saturation point under normoxia leading to cell death, whereas under hypoxia, autophagy flow still correctly took place allowing the cells to survive. The conclusion was reached using several experimental approaches as well as using detailed time curves. When looking at only 16 h of incubation in the presence of taxol, no difference in LC3II abundance under hypoxia as compared to normoxia was observed, as shown here (Figs. 3, 6 and 7). In this previous study, we showed that the inhibition of the taxol-induced activation of autophagy led to an increase in cytotoxicity and in the current study, the decrease in LC3II accumulation observed in response to ATF4 silencing also led to an increase in cytotoxicity. In conclusion, ATF4 is necessary for an effective autophagic process during taxol exposure. These results are in accordance with previous reports from Rouschop et al. (Rouschop et al., 2010) and Rzymski et al. (Rzymski et al., 2009; Milani et al., 2009; Rzymski et al., 2010) demonstrating that ATF4 transcriptionally regulates LC3 expression allowing a continuous supply of this protein for

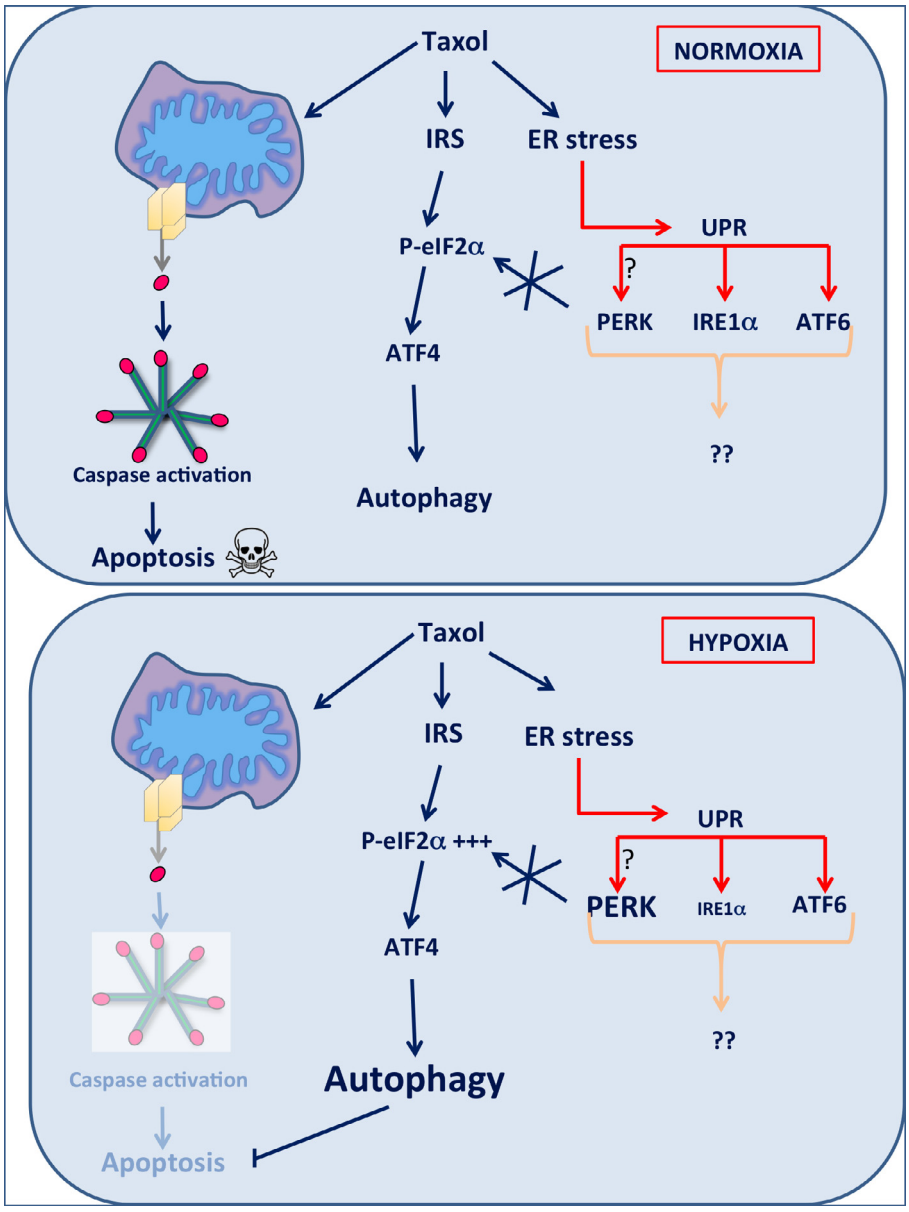

Fig. 9. Mechanisms promoting cancer cell survival after taxol treatment under hypoxia.
Taxol induces caspase activation and subsequent apoptosis and cell death in breast cancer cells. However, different mechanisms are activated to inhibit taxol-induced apoptosis activation. We showed that taxol induces an ER stress leading to activation of the three ER-stress sensors and UPR activation. UPR activation is neither involved in autophagy activation, nor in apoptosis inhibition after taxol incubation. However, after taxol exposure, autophagy is activated in an ATF4-dependent way that promotes cell survival against taxol-induced cell death both under normoxia and hypoxia.

an effective autophagic process. However, these studies were performed under severe hypoxia or after the inhibition of the 26S proteasome by Bortezomib. Rouschop et al. also showed that ATF4 activation under severe hypoxia was dependent on PERK activation whereas Rzymski et al. showed that ATF4 activation after Bortezomib treatment was PERK-independent.

ATF4 is a mediator of the integrated stress response (ISR) and is activated downstream of eIF2α phosphorylation (Ameri and Harris, 2008). Three kinases other than PERK are able to phosphorylate eIF2α during the ISR: GCN2, PKR, and HRI. Yerlikaya et al. showed that Bortezomib or MG-231 activates HRI. (Yerlikaya et al., 2008) ATF4 dependent-autophagy activation in response to proteasome inhibition could be due to HRI activation. In our work, taxol-induced ATF4 activation could also be PERK-independent since invalidation of PERK with siRNA did not influence autophagy nor apoptosis activation. By silencing the three ISR kinases, HRI, PKR, or GCN2, we showed that the kinase responsible for ATF4 induction is HRI.

In conclusion, different mechanisms promoting breast cancer cell adaptation to hypoxia and resistance against taxol-induced apoptosis were highlighted (Fig. 9). We showed that taxol-induced UPR activation is neither involved in autophagy nor in apoptosis activation. On the other hand, ATF4 promotes cancer cell survival under basal conditions and after taxol exposure. ATF4 also allows LC3I to LC3II conversion and autophagy completion suggesting that ATF4 is important for autophagosome elongation and autophagy execution that promotes resistance against taxol-induced cell death. Autophagy regulation by ATF4 seems to be independent of PERK activation and seems to occur through the activation of the ISR via the HRI kinase. Moreover, ATF4 is described to be expressed at higher level in cancer when compared to normal tissue (Ameri et al., 2004), this may be due to the induction of its

expression by signals specific to the tumor microenvironment such as hypoxia, nutrient deprivation, oxidative stress, and/or ER stress.

Finally, breast cancer patients carrying the ATF4^{high}/ADM^{high} had a lower survival probably compared to breast cancer patients with low expression of these genes. This result suggests that ATF4 expression might be associated with hypoxia cell response. This molecular signature could thus be used as a biomarker reflecting a poor prognosis in human breast cancer. This further supports the conclusion that ATF4 plays a role in the adaptation and resistance of breast cancer cells against chemotherapy.

Conflict of interest statement

The authors declare no conflict of interest.

Acknowledgments

We acknowledge Professor J.Y. Shyy (University of California, Riverside, CA, USA) for generously providing the ATF6/XBP1 luciferase reporter plasmid. A. Notte and C. Tellier are PhD fellows from FNRS (National Funds for Scientific Research, Brussels, Belgium). M. Genin benefits from a PhD grant from FRIA (FNRS, Brussels, Belgium) and M. Rebucci and E. Roegiers are respectively a post-doctoral researcher and a PhD grantee from Televie (FNRS, Brussels, Belgium).

Appendix A. Supplementary data

Supplementary data associated with this article can be found, in the online version, at http://dx.doi.org/10.1016/j.biocel.2015.02.010.

References

Ameri K, Harris AL. Activating transcription factor 4. Int J Biochem Cell Biol 2008;40(1):14–21.
Ameri K, Lewis CE, Raida M, Sowter H, Hai T, Harris AL. Anoxic induction of ATF-4 through HIF-1-independent pathways of protein stabilization in human cancer cells. Blood 2004;103(5):1876–82.
Bertolotti A, Zhang Y, Hendershot LM, Harding HP, Ron D. Dynamic interaction of BiP and ER stress transducers in the unfolded-protein response. Nat Cell Biol 2000;2(6):326–32.
Bi M, Naczki C, Koritzinsky M, Fels D, Blais J, Hu N, et al. ER stress-regulated translation increases tolerance to extreme hypoxia and promotes tumor growth. EMBO J 2005;24(19):3470–81.
Brahimi-Horn C, Pouyssegur J. The role of the hypoxia-inducible factor in tumor metabolism growth and invasion. B Cancer 2006;93(8):E73–80.
Bravo R, Parra V, Gatica D, Rodriguez AE, Torrealba N, Paredes F, et al. Endoplasmic reticulum and the unfolded protein response: dynamics and metabolic integration. Int Review Cell Mol Biol 2013;301:215–90.
Chakrabarti A, Chen AW, Varner JD. A review of the mammalian unfolded protein response. Biotechnol Bioeng 2011;108(12):2777–93.
Checinska A, Soengas MS. The gluttonous side of malignant melanoma: basic and clinical implications of macroautophagy. Pigment Cell Melanoma Res 2011;24(6):1116–32.
Chen R, Dai RY, Duan CY, Liu YP, Chen SK, Yan DM, et al. Unfolded protein response suppresses cisplatin-induced apoptosis via autophagy regulation in human hepatocellular carcinoma cells. Folia Biol 2011;57(3):87–95.
Codogno P, Meijer AJ. Autophagy and signaling: their role in cell survival and cell death. Cell Death Differ 2005;12(Suppl 2):1509–18.
Deegan S, Saveljeva S, Gorman AM, Samali A. Stress-induced self-cannibalism: on the regulation of autophagy by endoplasmic reticulum stress. Cell Mol Life Sci 2012.
Donnelly N, Gorman AM, Gupta S, Samali A. The eIF2alpha kinases: their structures and functions. Cell Mol Life Sci 2013.
Feng R, Zhai WL, Yang HY, Jin H, Zhang QX. Induction of ER stress protects gastric cancer cells against apoptosis induced by cisplatin and doxorubicin through activation of p38 MAPK. Biochem Bioph Res Co 2011;406(2):299–304.
Garcia-Navas R, Munder M, Mollinedo F. Depletion of L-arginine induces autophagy as a cytoprotective response to endoplasmic reticulum stress in human T lymphocytes. Autophagy 2012;8(11):1557–76.
Gatti L, Zunino F. Overview of tumor cell chemoresistance mechanisms. Methods Mol Med 2005;111:127–48.
Harding HP, Novoa I, Zhang Y, Zeng H, Wek R, Schapira M, et al. Regulated translation initiation controls stress-induced gene expression in mammalian cells. Mol Cell 2000;6(5):1099–108.
He C, Klionsky DJ. Regulation mechanisms and signaling pathways of autophagy. Annu Rev Genet 2009;43:67–93.
Healy SJ, Gorman AM, Mousavi-Shafaei P, Gupta S, Samali A. Targeting the endoplasmic reticulum-stress response as an anticancer strategy. Eur J Pharmacol 2009;625(1–3):234–46.
Heath-Engel HM, Chang NC, Shore GC. The endoplasmic reticulum in apoptosis and autophagy: role of the BCL-2 protein family. Oncogene 2008;27(50):6419–33.
Hoyer-Hansen M, Jaattela M. Connecting endoplasmic reticulum stress to autophagy by unfolded protein response and calcium. Cell Death Diff 2007;14(9):1576–82.
Ivshina AV, George J, Senko O, Mow B, Putti TC, Smeds J, et al. Genetic reclassification of histologic grade delineates new clinical subtypes of breast cancer. Cancer Res 2006;66(21):10292–301.
Jiang CC, Lucas K, Avery-Kiejda KA, Wade M, deBock CE, Thorne RF, et al. Up-regulation of Mcl-1 is critical for survival of human melanoma cells upon endoplasmic reticulum stress. Cancer Res 2008;68(16):6708–17.
Kiviluoto S, Vervliet T, Ivanova H, Decuypere JP, De Smedt H, Missiaen L, et al. Regulation of inositol 1,4,5-trisphosphate receptors during endoplasmic reticulum stress. Biochim Biophys Acta 2013;1833(7):1612–24.
Koumenis C. ER stress, hypoxia tolerance and tumor progression. Curr Mol Med 2006;6(1):55–69.
Kouroku Y, Fujita E, Tanida I, Ueno T, Isoai A, Kumagai H, et al. ER stress (PERK/eIF2alpha phosphorylation) mediates the polyglutamine-induced LC3 conversion, an essential step for autophagy formation. Cell Death Differ 2007;14(2):230–9.
Kumandan S, Mahadevan NR, Chiu K, DeLaney A, Zanetti M. Activation of the unfolded protein response bypasses trastuzumab-mediated inhibition of the PI-3K pathway. Cancer Lett 2013;329(2):236–42.
Lassot I, Segeral E, Berlioz-Torrent C, Durand H, Groussin L, Hai T, et al. ATF4 degradation relies on a phosphorylation-dependent interaction with the SCF(betaTrCP) ubiquitin ligase. Mol Cell Biol 2001;21(6):2192–202.
Li J, Lee AS. Stress induction of GRP78/BiP and its role in cancer. Curr Mol Med 2006;6(1):45–54.
Liao PC, Tan SK, Lieu CH, Jung HK. Involvement of endoplasmic reticulum in paclitaxel-induced apoptosis. J Cell Biochem 2008;104(4):1509–23.
Lozano J, Menendez S, Morales A, Ehleiter D, Liao WC, Wagman R, et al. Cell autonomous apoptosis defects in acid sphingomyelinase knockout fibroblasts. J Biol Chem 2001;276(1):442–8.
Lu L, Han AP, Chen JJ. Translation initiation control by heme-regulated eukaryotic initiation factor 2alpha kinase in erythroid cells under cytoplasmic stresses. Mol Cell Biol 2001;21(23):7971–80.
Mann MJ, Hendershot LM. UPR activation alters chemosensitivity of tumor cells. Cancer Biol Ther 2006;5(7):736–40.
McCullough KD, Martindale JL, Klotz LO, Aw TY, Holbrook NJ. Gadd153 sensitizes cells to endoplasmic reticulum stress by down-regulating Bcl2 and perturbing the cellular redox state. Mol Cell Biol 2001;21(4):1249–59.
Mehrpour M, Esclatine A, Beau I, Codogno P. Overview of macroautophagy regulation in mammalian cells. Cell Res 2010;20(7):748–62.
Milani M, Rzymski T, Mellor HR, Pike L, Bottini A, Generali D, et al. The role of ATF4 stabilization and autophagy in resistance of breast cancer cells treated with Bortezomib. Cancer Res 2009;69(10):4415–23.
Morselli E, Galluzzi L, Kepp O, Vicencio JM, Criollo A, Maiuri MC, et al. Anti- and pro-tumor functions of autophagy. Biochim Biophys Acta 2009;1793(9):1524–32.
Nishitoh H, Matsuzawa A, Tobiume K, Saegusa K, Takeda K, Inoue K, et al. ASK1 is essential for endoplasmic reticulum stress-induced neuronal cell death triggered by expanded polyglutamine repeats. Genes Dev 2002;16(11):1345–55.
Notte A, Leclere L, Michiels C. Autophagy as a mediator of chemotherapy-induced cell death in cancer. Biochem Pharmacol 2011;82(5):427–34.
Notte A, Ninane N, Arnould T, Michiels C. Hypoxia counteracts taxol-induced apoptosis in MDA-MB-231 breast cancer cells: role of autophagy and JNK activation. Cell Death Dis 2013;4:e638.
Ogata M, Hino S, Saito A, Morikawa K, Kondo S, Kanemoto S, et al. Autophagy is activated for cell survival after endoplasmic reticulum stress. Mol Cell Biol 2006;26(24):9220–31.
Ohoka N, Yoshii S, Hattori T, Onozaki K, Hayashi H. TRB3, a novel ER stress-inducible gene, is induced via ATF4-CHOP pathway and is involved in cell death. EMBO J 2005;24(6):1243–55.
Oyadomari S, Mori M. Roles of CHOP/GADD153 in endoplasmic reticulum stress. Cell Death Diff 2004;11(4):381–9.
Pan Y, Xiao J, Liang G, Wang M, Wang D, Wang S, et al. A new curcumin analogue exhibits enhanced antitumor activity in nasopharyngeal carcinoma. Oncol Rep 2013;30(1):239–45.
Pierre M, DeHertogh B, Gaigneaux A, DeMeulder B, Berger F, Bareke E, et al. Meta-analysis of archived DNA microarrays identifies genes regulated by hypoxia and involved in a metastatic phenotype in cancer cells. BMC Cancer 2010;10:176.
Rasheva VI, Domingos PM. Cellular responses to endoplasmic reticulum stress and apoptosis. Apoptosis 2009;14(8):996–1007.
Rohwer N, Cramer T. Hypoxia-mediated drug resistance: novel insights on the functional interaction of HIFs and cell death pathways. Drug Resist Updat 2011;14(3):191–201.
Romero-Ramirez L, Cao H, Nelson D, Hammond E, Lee AH, Yoshida H, et al. XBP1 is essential for survival under hypoxic conditions and is required for tumor growth. Cancer Res 2004;64(17):5943–7.

Ron D, Walter P. Signal integration in the endoplasmic reticulum unfolded protein response. Nat Rev Mol Cell Biol 2007;8(7):519–29.
Rouschop KM, Wouters BG. Regulation of autophagy through multiple independent hypoxic signaling pathways. Curr Mol Med 2009;9(4):417–24.
Rouschop KM, van den Beucken T, Dubois L, Niessen H, Bussink J, Savelkouls K, et al. The unfolded protein response protects human tumor cells during hypoxia through regulation of the autophagy genes MAP1LC3B and ATG5. J Clin Invest 2010;120(1):127–41.
Rzymski T, Milani M, Singleton DC, Harris AL. Role of ATF4 in regulation of autophagy and resistance to drugs and hypoxia. Cell Cycle 2009;8(23):3838–47.
Rzymski T, Milani M, Pike L, Buffa F, Mellor HR, Winchester L, et al. Regulation of autophagy by ATF4 in response to severe hypoxia. Oncogene 2010;29(31):4424–35.
Schonthal AH. Pharmacological targeting of endoplasmic reticulum stress signaling in cancer. Biochem Pharmacol 2013;85(5):653–66.
Semenza GL. HIF-1: upstream and downstream of cancer metabolism. Curr Opin Genet Dev 2010;20(1):51–6.
Shajahan AN, Riggins RB, Clarke R. The role of X-box binding protein-1 in tumorigenicity. Drug News Perspect 2009;22(5):241–6.
Shannon AM, Bouchier-Hayes DJ, Condron CM, Toomey D. Tumour hypoxia, chemotherapeutic resistance and hypoxia-related therapies. Cancer Treat Rev 2003;29(4):297–307.
Shen J, Chen X, Hendershot L, Prywes R. ER stress regulation of ATF6 localization by dissociation of BiP/GRP78 binding and unmasking of Golgi localization signals. Dev Cell 2002;3(1):99–111.
Shen S, Kepp O, Kroemer G. The end of autophagic cell death? Autophagy 2012;8(1):1–3.
Song J, Qu Z, Guo X, Zhao Q, Zhao X, Gao L, et al. Hypoxia-induced autophagy contributes to the chemoresistance of hepatocellular carcinoma cells. Autophagy 2009;5(8):1131–44.
Szegezdi E, Logue SE, Gorman AM, Samali A. Mediators of endoplasmic reticulum stress-induced apoptosis. EMBO Rep 2006;7(9):880–5.
Szegezdi E, Macdonald DC, Ni Chonghaile T, Gupta S, Samali A. Bcl-2 family on guard at the ER. Am J Physiol Cell Physiol 2009;296(5):C941–53.
Travers KJ, Patil CK, Wodicka L, Lockhart DJ, Weissman JS, Walter P. Functional and genomic analyses reveal an essential coordination between the unfolded protein response and ER-associated degradation. Cell 2000;101(3):249–58.
Urano F, Wang X, Bertolotti A, Zhang Y, Chung P, Harding HP, et al. Coupling of stress in the ER to activation of JNK protein kinases by transmembrane protein kinase IRE1. Science 2000;287(5453):664–6.
Vannuvel K, Renard P, Raes M, Arnould T. Functional and morphological impact of ER stress on mitochondria. J Cellular Physio 2013;228(9):1802–18.
Walter P, Ron D. The unfolded protein response: from stress pathway to homeostatic regulation. Science 2011;334(6059):1081–6.
Wang J, Yin Y, Hua H, Li M, Luo T, Xu L, et al. Blockade of GRP78 sensitizes breast cancer cells to microtubules-interfering agents that induce the unfolded protein response. J Cell Mol Med 2009;13(9B):3888–97.
Wellington CL, Ellerby LM, Hackam AS, Margolis RL, Trifiro MA, Singaraja R, et al. Caspase cleavage of gene products associated with triplet expansion disorders generates truncated fragments containing the polyglutamine tract. J Biol Chem 1998;273(15):9158–67.
White E. Deconvoluting the context-dependent role for autophagy in cancer. Nat Rev Cancer 2012;12(6):401–10.
Winter SC, Buffa FM, Silva P, Miller C, Valentine HR, Turley H, et al. Relation of a hypoxia metagene derived from head and neck cancer to prognosis of multiple cancers. Cancer Res 2007;67(7):3441–9.
Ye J, Koumenis C. ATF4, an ER stress and hypoxia-inducible transcription factor and its potential role in hypoxia tolerance and tumorigenesis. Curr Mol Med 2009;9(4):411–6.
Yerlikaya A, Kimball SR, Stanley BA. Phosphorylation of eIF2alpha in response to 26S proteasome inhibition is mediated by the haem-regulated inhibitor (HRI) kinase. Biochem J 2008;412(3):579–88.
Yorimitsu T, Klionsky DJ. Eating the endoplasmic reticulum: quality control by autophagy. Trends Cell Biol 2007;17(6):279–85.
Yu S, Zhu K, Lai Y, Zhao Z, Fan J, Im HJ, et al. atf4 promotes beta-catenin expression and osteoblastic differentiation of bone marrow mesenchymal stem cells. Int J Biol Sci 2013;9(3):256–66.
Zeng L, Lu M, Mori K, Luo S, Lee AS, Zhu Y, et al. ATF6 modulates SREBP2-mediated lipogenesis. EMBO J 2004;23(4):950–8.
Zhang H, Bosch-Marce M, Shimoda LA, Tan YS, Baek JH, Wesley JB, et al. Mitochondrial autophagy is an HIF-1-dependent adaptive metabolic response to hypoxia. J Biol Chem 2008;283(16):10892–903.